

Gauge dependence of fermion mass renormalization schemes

Yong Zhou

*Institute of High Energy Physics, Academia Sinica,
P.O. Box 918(4), Beijing 100049, China, Email: zhouy@ihep.ac.cn*

We discuss the gauge dependence of fermion mass definition and physical result under the conventional on-shell mass renormalization scheme and the recently proposed pole mass renormalization scheme in standard model. By the two-loop calculations of top quark's mass counterterm and the cross section of physical process $W^-W^+ \rightarrow b\bar{b}$ we strictly prove that the on-shell mass renormalization scheme makes fermion mass definition and the physical result gauge dependent at the first time, while we don't find such gauge dependence in the pole mass renormalization scheme. Besides, our calculation also shows the difference of the physical result between the two mass renormalization schemes cannot be neglected at two-loop level.

PACS numbers: 11.10.Gh, 12.15.Ff, 12.15.Lk

I. INTRODUCTION

Along with the improvement of the measurement precision of physical experiments, we need more and more radiative-correction calculations beyond one-loop level. The fermion mass renormalization scheme has been discussed enough at one-loop level [1, 2], but is rarely discussed beyond one-loop level. At present there are two mass renormalization schemes: the conventional on-shell scheme [1, 2] and the recently proposed pole scheme [3]. People have pointed out that the mass definition of pole scheme is gauge invariant compared with the on-shell scheme [3, 4], but this conclusion is only based on a native hypothesis that the location of the complex pole of the propagator is gauge independent at any order in perturbation theory [5] and a strict proof of the hypothesis hasn't been present. So we need to further investigate this problem. In this paper we will investigate the gauge dependence of fermion mass definition.

In order to obtain the fermion mass renormalization scheme beyond one-loop level we firstly investigate the fermion inverse propagator

$$iS^{-1}(\not{p}) = \not{p} - m_0 + \Sigma(\not{p}) \equiv \not{p}(a\gamma_L + b\gamma_R) + c\gamma_L + d\gamma_R, \quad (1)$$

where m_0 is the bare fermion mass, γ_L and γ_R are the left- and right- handed helicity operators, and

$$\Sigma(\not{p}) = \not{p}\gamma_L \Sigma^L(p^2) + \not{p}\gamma_R \Sigma^R(p^2) + m\gamma_L \Sigma^{S,L}(p^2) + m\gamma_R \Sigma^{S,R}(p^2). \quad (2)$$

When we renormalize fermion mass, the fermion propagator should be changed into [1, 6]

$$S(\not{p}) = \frac{\not{p}(a\gamma_L + b\gamma_R) - d\gamma_L - c\gamma_R}{p^2 ab - cd} = \frac{i(m_0 + \not{p}\gamma_L(1 + \Sigma^L) + \not{p}\gamma_R(1 + \Sigma^R) - m\gamma_L \Sigma^{S,R} - m\gamma_R \Sigma^{S,L})}{p^2(1 + \Sigma^L)(1 + \Sigma^R) - (m_0 - m\Sigma^{S,L})(m_0 - m\Sigma^{S,R})}. \quad (3)$$

The on-shell mass renormalization scheme requires the real part of the propagator's denominator equal to zero at the physical mass point, i.e. [6]

$$Re[m^2(1 + \Sigma^L(m^2))(1 + \Sigma^R(m^2)) - (m + \delta m - m\Sigma^{S,L}(m^2))(m + \delta m - m\Sigma^{S,R}(m^2))] = 0. \quad (4)$$

Solving this equation about δm to two-loop level we obtain

$$\begin{aligned} \delta m = & \frac{m}{2} Re[\Sigma^L(m^2) + \Sigma^R(m^2) + \Sigma^{S,L}(m^2) + \Sigma^{S,R}(m^2)] - \frac{m}{8} Re^2[\Sigma^L(m^2) - \Sigma^R(m^2)] \\ & + \frac{m}{2} (Im\Sigma^{S,L}(m^2)Im\Sigma^{S,R}(m^2) - Im\Sigma^L(m^2)Im\Sigma^R(m^2)). \end{aligned} \quad (5)$$

In Eq.(5) we have used the fact $\Sigma^{S,L} = \Sigma^{S,R}$ at one-loop level.

Different from the on-shell scheme, the pole mass renormalization scheme requires both the real part and the imaginary part of the propagator's denominator equal to zero at the location of the propagator's complex pole [7]

$$\bar{s}(1 + \Sigma^L(\bar{s}))(1 + \Sigma^R(\bar{s})) - (m_2 + \delta m_2 - m_2\Sigma^{S,L}(\bar{s}))(m_2 + \delta m_2 - m_2\Sigma^{S,R}(\bar{s})) = 0, \quad (6)$$

where m_2 is the physical mass and $\bar{s} = m_2^2 - im_2\Gamma_2$ is the location of the propagator's complex pole. Solving this equation about δm_2 to two-loop level we obtain

$$\begin{aligned} \delta m_2 = & \frac{m_2}{2} \text{Re}[\Sigma^L(m_2^2) + \Sigma^R(m_2^2) + \Sigma^{S,L}(m_2^2) + \Sigma^{S,R}(m_2^2)] - \frac{m_2}{8} \text{Re}^2[\Sigma^L(m_2^2) - \Sigma^R(m_2^2)] \\ & + \frac{m_2}{2} (\text{Im}\Sigma^{S,L}(m_2^2)\text{Im}\Sigma^{S,R}(m_2^2) - \text{Im}\Sigma^L(m_2^2)\text{Im}\Sigma^R(m_2^2)) \\ & + \frac{\Gamma_2}{2} (m_2^2 \text{Im}[\Sigma^{L'}(m_2^2) + \Sigma^{R'}(m_2^2) + \Sigma^{S,L'}(m_2^2) + \Sigma^{S,R'}(m_2^2)] + \text{Im}[\Sigma^L(m_2^2) + \Sigma^R(m_2^2)]), \end{aligned} \quad (7)$$

where $\Sigma^{L'}(m_2^2) = \partial\Sigma^L(m_2^2)/\partial p^2$ et al and the one-loop fermion decay width Γ_2 is

$$\Gamma_2 = m_2 \text{Im}[\Sigma^L(m_2^2) + \Sigma^R(m_2^2) + \Sigma^{S,L}(m_2^2) + \Sigma^{S,R}(m_2^2)]. \quad (8)$$

In order to investigate the gauge dependence of the two fermion mass definitions we calculate the gauge dependence of the branch cut of top quark's two-loop mass counterterm in the following section; in section III we calculate the cross section of the physical process $W^-W^+ \rightarrow b\bar{b}$, i.e. a pair of gauge boson W decaying into a pair of bottom quarks, to investigate the gauge dependence of physical result under the on-shell mass renormalization scheme; lastly we give the conclusion in section IV.

II. GAUGE DEPENDENCE OF FERMION MASS DEFINITION IN THE ON-SHELL AND POLE MASS RENORMALIZATION SCHEMES

If fermion mass is defined gauge independently, its counterterm must be also gauge independent [8]. This can be used to test whether the fermion mass definition is gauge independent. In the following calculations we will investigate whether Eq.(5) and Eq.(7) are gauge independent. For convenience we only consider W gauge parameter's dependence in the R_ξ gauge and only introduce physical parameter's counterterms. Note that we have used the computer program packages *FeynArts* and *FeynCalc* [9] in the following calculations.

We give top quark's mass counterterm as an example to investigate this problem. Since nobody has discussed this problem before, we begin the discussion from the one-loop level. The one-loop top quark's ξ_W -dependent self-energy and tadpole diagrams are shown in Fig.1 and Fig.2, where ξ_W is W gauge parameter. We note that in order to investigate the gauge dependence of mass counterterm the tadpole diagrams of Fig.2 must be included [5]. We firstly

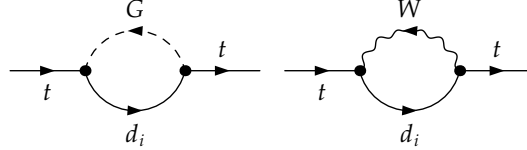


FIG. 1: Diagrams of one-loop top quark's ξ_W -dependent self energy.

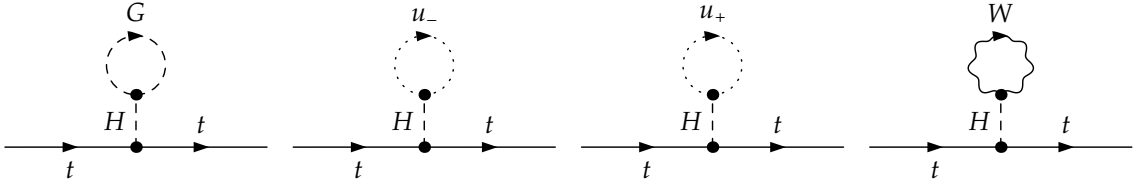


FIG. 2: Tadpole diagrams of one-loop top quark's ξ_W -dependent self energy.

obtain the ξ_W -dependent contribution of Fig.1 to top quark's one-loop mass counterterm (see Eqs.(5,7))

$$\frac{m_t}{2} \text{Re}[\Sigma^L(m_t^2) + \Sigma^R(m_t^2) + \Sigma^{S,L}(m_t^2) + \Sigma^{S,R}(m_t^2)]_{\xi_W} = \frac{e^2 m_t}{64\pi^2 s_w^2} \xi_W (1 + B_0(0, \xi_W m_W^2, \xi_W m_W^2)), \quad (9)$$

where the subscript ξ_W denotes the ξ_W -dependent part of the quantity, m_t and m_W are the masses of top quark and gauge boson W, e is electron charge, s_w is the sine of weak mixing angle, and B_0 is the Passarino-Veltman function [10]. On the other hand, the ξ_W -dependent contribution of Fig.2 to top quark's one-loop mass counterterm is

$$\frac{m_t}{2} \text{Re}[\Sigma^L(m_t^2) + \Sigma^R(m_t^2) + \Sigma^{S,L}(m_t^2) + \Sigma^{S,R}(m_t^2)]_{\xi_W} = -\frac{e^2 m_t}{64\pi^2 s_w^2} \xi_W (1 + B_0(0, \xi_W m_W^2, \xi_W m_W^2)). \quad (10)$$

From Eqs.(9,10) one readily see that the top quark's one-loop mass counterterm is gauge independent.

Now we calculate the gauge dependence of top quark's two-loop mass counterterm. For convenience we only calculate the gauge dependence of the branch cut of top quark's mass counterterm. Since the gauge-dependent branch cut of top quark's mass counterterm comprises gauge-dependent Heaviside function only (see below) and the other part of top quark's mass counterterm doesn't contain such function, this simplified treatment is reasonable and will not break our final conclusion. The branch cut of top quark's two-loop mass counterterm will be calculated by the *cutting rules* [11, 12]. The concrete algorithm used here can be found in Ref.[12]. From Eqs.(5,7) we find at two-loop level the top quark's mass counterterms are different in the two mass renormalization schemes. We firstly discuss the case of on-shell mass renormalization scheme. It is obvious that at two-loop level the second term of the r.h.s. of Eq.(5) doesn't contain branch cut. So we don't need to consider this term. Through the imaginary part of Fig.1 we obtain the ξ_W -dependent branch cut of the last term of the r.h.s. of Eq.(5)

$$\begin{aligned} & \frac{m_t}{2} [Im\Sigma^{S,L}(m_t^2)Im\Sigma^{S,R}(m_t^2) - Im\Sigma^L(m_t^2)Im\Sigma^R(m_t^2)]_{\xi_W-cut} \\ &= -\frac{e^4 m_W}{8192\pi^2 s_w^4 x_t^{5/2}} \sum_{i=d,s,b} |V_{3i}|^2 A_i C_i \sum_{j=d,s,b} |V_{3j}|^2 B_j (x_t - \xi_W + x_j) \theta[m_t - m_j - \sqrt{\xi_W m_W}] \\ &+ \frac{e^4 m_W}{8192\pi^2 s_w^4 x_t^{3/2}} \sum_{i,j=d,s,b} |V_{3i}|^2 |V_{3j}|^2 B_i B_j ((x_t - \xi_W)(x_t - \xi_W - 3x_i) + (x_t - \xi_W + x_i)x_j) \\ &\times \theta[m_t - m_i - \sqrt{\xi_W m_W}] \theta[m_t - m_j - \sqrt{\xi_W m_W}], \end{aligned} \quad (11)$$

where the subscript ξ_W-cut denotes the ξ_W -dependent branch cut of the quantity, V_{3i} and V_{3j} are CKM matrix elements [13], m_i and m_j are the masses of down-type i and j quarks, $x_t = m_t^2/m_W^2$, $x_i = m_i^2/m_W^2$ and $x_j = m_j^2/m_W^2$, θ is the Heaviside function, and

$$\begin{aligned} A_i &= (x_t^2 - 2(x_i + 1)x_t + (x_i - 1)^2)^{1/2}, \\ B_i &= (x_t^2 - 2(\xi_W + x_i)x_t + (\xi_W - x_i)^2)^{1/2}, \\ C_i &= x_t^2 + (1 - 2x_i)x_t + x_i^2 + x_i - 2. \end{aligned} \quad (12)$$

In order to investigate the gauge dependence of the branch cut of the first term of the r.h.s. of Eq.(5) we need to calculate top quark's two-loop self energy. The top quark's two-loop self energy can be classified into two kinds: one contains the one-loop counterterm, the second doesn't contain any counterterm. Since except for CKM matrix elements all the one-loop physical parameter's counterterms are real numbers and free of branch cut [2], the first kind self energy doesn't contribute to the branch cut of Eq.(5), because except the one-loop counterterm the left part of the self energy is the one-loop self energy which real part is free of branch cut. Here we don't need to worry about the problem of the CKM matrix elements and their counterterms being complex numbers, because the total contribution of them to Eq.(5) is real number (see the appendix for example). So we only need to consider the second kind self energy. According to the *cutting rules* of Ref.[12], the second kind self energy can also be classified into three kinds: one doesn't contain branch cut, the second contains branch cut, but its branch cut doesn't contribute to Eq.(5), the third contains branch cut and its branch cut contributes to Eq.(5) [14]. Obviously only the third kind self energy needs to be calculated. The topologies of it are shown in Fig.3 [14]. One notices in Fig.3 that an one-particle-reducible diagram has been included. Although a self energy is usually defined to comprise one-particle-irreducible diagrams only, no physical principle demonstrates the one-particle-reducible diagram can not be included in a correct self energy. Furthermore in the following calculations of top quark's mass counterterm one will see the one-particle-reducible diagram in Fig.3 guarantees the gauge independence of the branch cut of top quark's mass definition under the p1e mass renormalization scheme. In Fig.3 we also draw the possible cuts of the first four topologies which contribute to Eq.(5), where the propagator with an arrow on it denotes it is cut and the arrow represents the *positive-on-shell* momentum propagating direction of the cut propagator [12]). The possible cuts of the left two topologies which contribute to Eq.(5) are shown in Fig.4 and Fig.5. The concrete calculations of the ξ_W -dependent contribution of the possible cuts of Fig.3 to Eq.(5) are shown in the appendix. Here we list the final

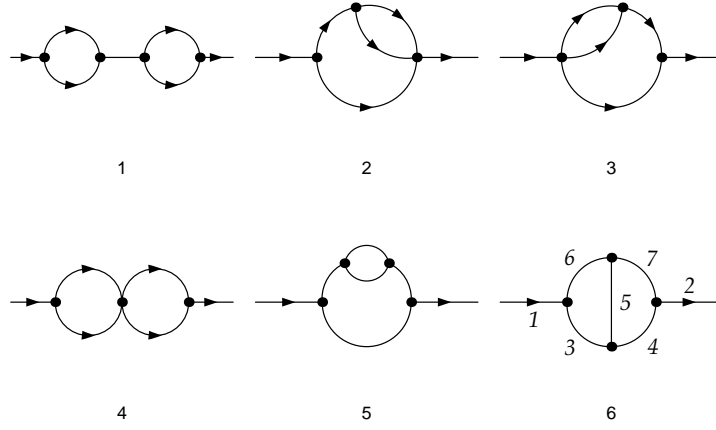


FIG. 3: Topologies of two-loop self energy without counterterm which branch cuts contribute to Eq.(5).

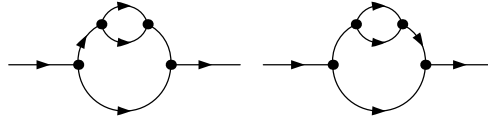


FIG. 4: Possible cuts of the 5th topology of Fig.3 which contribute to Eq.(5).

result

$$\begin{aligned}
& \frac{m_t}{2} \text{Re}[\Sigma^L(m_t^2) + \Sigma^R(m_t^2) + \Sigma^{S,L}(m_t^2) + \Sigma^{S,R}(m_t^2)]_{\xi_W - \text{cut}} \\
&= \frac{e^4 m_W}{4096 \pi^2 s_w^4 x_t^{5/2}} \sum_{i=d,s,b} |V_{3i}|^2 A_i C_i \sum_{j=d,s,b} |V_{3j}|^2 B_j (x_t - \xi_W - x_j) \theta[m_t - m_j - \sqrt{\xi_W m_W}] \\
&- \frac{e^4 m_W}{8192 \pi^2 s_w^4 x_t^{3/2}} \sum_{i,j=d,s,b} |V_{3i}|^2 |V_{3j}|^2 B_i B_j (x_t - \xi_W - x_i)(x_t - \xi_W - x_j) \\
&\times \theta[m_t - m_i - \sqrt{\xi_W m_W}] \theta[m_t - m_j - \sqrt{\xi_W m_W}]. \tag{13}
\end{aligned}$$

From Eq.(5) and Eqs.(11,13) we obtain the gauge dependence of the branch cut of top quark's two-loop mass

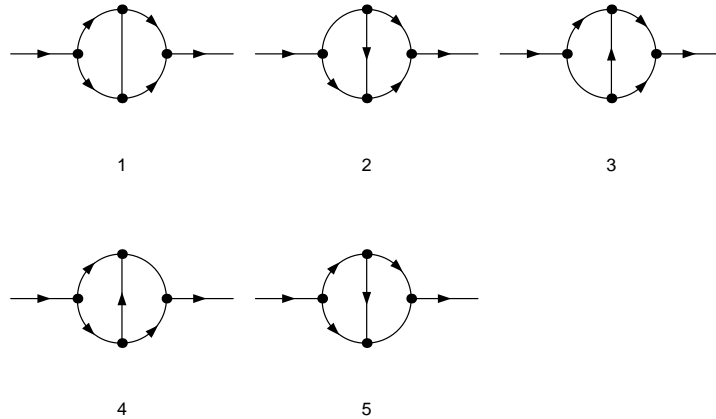


FIG. 5: Possible cuts of the 6th topology of Fig.3 which contribute to Eq.(5).

counterterm under the on-shell mass renormalization scheme

$$\delta m_t|_{\xi_W - cut} = \frac{e^4 m_W}{8192\pi^2 s_w^4 x_t^{5/2}} \sum_{i=d,s,b} |V_{3i}|^2 A_i C_i \sum_{j=d,s,b} |V_{3j}|^2 B_j (x_t - \xi_W - 3x_j) \theta[m_t - m_j - \sqrt{\xi_W m_W}]. \quad (14)$$

According to the above discussion above Eqs.(11) Eq.(14) manifests top quark's two-loop mass counterterm is gauge dependent under the on-shell mass renormalization prescription. This means the conventional on-shell mass definition is gauge dependent according to the discussion at the beginning of this section.

Then we calculate the gauge dependence of top quark's two-loop mass counterterm under the pole mass renormalization scheme. The result of the first three terms of Eq.(7) is same as the result of Eq.(5). So we only need to calculate the last term of Eq.(7). The concrete result is

$$\begin{aligned} & \frac{\Gamma_t}{2} (m_t^2 \text{Im}[\Sigma^{L'}(m_t^2) + \Sigma^{R'}(m_t^2) + \Sigma^{S,L'}(m_t^2) + \Sigma^{S,R'}(m_t^2)] + \text{Im}[\Sigma^L(m_t^2) + \Sigma^R(m_t^2)])|_{\xi_W - cut} \\ &= -\frac{e^4 m_W}{8192\pi^2 s_w^4 x_t^{5/2}} \sum_{i=d,s,b} |V_{3i}|^2 A_i C_i \sum_{j=d,s,b} |V_{3j}|^2 B_j (x_t - \xi_W - 3x_j) \theta[m_t - m_j - \sqrt{\xi_W m_W}]. \end{aligned} \quad (15)$$

From Eq.(7) and Eqs.(11,13,15) we readily have

$$\delta m_t|_{\xi_W - cut} = 0. \quad (16)$$

This means in the pole mass definition we don't find the gauge dependence present in the on-shell mass definition.

III. GAUGE DEPENDENCE OF PHYSICAL RESULT UNDER THE ON-SHELL MASS RENORMALIZATION SCHEME

From the above discussion one readily sees that the conventional on-shell mass renormalization scheme is unreasonable. In fact the on-shell mass renormalization condition of Eq.(4) doesn't exist, because it requires the bare fermion mass m_0 is gauge dependent which is disallowed. In this section we will further discuss the effect of the gauge dependence of the on-shell fermion mass definition on physical result. We give the physical process $W^-W^+ \rightarrow b\bar{b}$ as an example to illustrate this problem. Note that we only consider the gauge dependence of the branch cut containing the function $\theta[m_t - m_{down-quark} - \sqrt{\xi_W m_W}]$ of the two-loop cross section of the physical process. For convenience we hypothesize the Higgs mass and the total energy of the incoming particles are less than top quark's mass. This will not break the following conclusion. Under the hypothesis only the diagram containing a two-loop δm_t needs to be consider. The contribution of Fig.6 to the two-loop amplitude $W^-W^+ \rightarrow b\bar{b}$ is

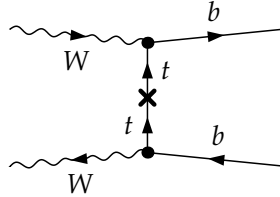


FIG. 6: Diagram of two-loop $W^-W^+ \rightarrow b\bar{b}$ containing a two-loop δm_t .

$$-\frac{e^2 |V_{33}|^2 m_t \delta m_t}{s_w^2 (m_b^2 + m_W^2 - 2p_2 \cdot q_2 - m_t^2)^2} [\bar{u}(q_1) \cdot \not{\epsilon}_1 \cdot \not{\epsilon}_2 \cdot \not{p}_2 \cdot \gamma_L \cdot \nu(q_2) + 2\bar{u}(q_1) \cdot \not{\epsilon}_1 \cdot \gamma_L \cdot \nu(q_2) \epsilon_2 \cdot q_2 + m_b \bar{u}(q_1) \cdot \not{\epsilon}_1 \cdot \not{\epsilon}_2 \cdot \gamma_R \cdot \nu(q_2)], \quad (17)$$

where m_b is bottom quark's mass, p_2 , q_1 and q_2 are the momentums of W^+ , bottom and anti-bottom quarks, and ϵ_1 and ϵ_2 are the polarization vectors of W^- and W^+ . The contribution of Eq.(17) to two-loop $|\mathcal{M}(W^-W^+ \rightarrow b\bar{b})|^2$ is

$$\begin{aligned} & \frac{e^4 |V_{33}|^2 m_t \delta m_t}{27m_W^2 s_w^4 (x_t + 2x_p - 1)^2} \left[-3(x_E(2x_p - 1)(2x_p + 1)^2 - 4x_p^2(4(x_p - 1)x_p + 5)) \sum_{i=u,c,t} \frac{|V_{i3}|^2}{2x_p + x_i - 1} \right. \\ & \left. + \frac{c_w^2(3x_E + 2) - 2}{x_E(c_w^2 x_E - 1)} (-8(x_E - 2)x_p^3 + 4(x_E - 3)(x_E + 2)x_p^2 + 4x_E^2 x_p - 3x_E(x_E + 2)) \right], \end{aligned} \quad (18)$$

where $x_p = p_2 \cdot q_2/m_W^2$ and $x_E = E_{cm}^2/m_W^2$ (E_{cm} is the total energy of the incoming particles in the center of mass frame). For convenience in Eq.(18) we have approximated $m_b^2/m_W^2 \rightarrow 0$ and averaged the result over the incoming particles' polarization vectors and summed the result over the outgoing particles' helicity states.

Since there is no other origin of function $\theta[m_t - m_{down-quark} - \sqrt{\xi_W}m_W]$ in the two-loop $|\mathcal{M}(W^-W^+ \rightarrow b\bar{b})|^2$, Eq.(14) and Eq.(18) mean the on-shell mass renormalization scheme makes the cross section of the physical process $W^-W^+ \rightarrow b\bar{b}$ gauge dependent. From Eqs.(14,18) we also find that the gauge dependence caused by the on-shell scheme cannot be neglected at two-loop level. The concrete numerical result is shown in Fig.7. In Fig.7 we have used

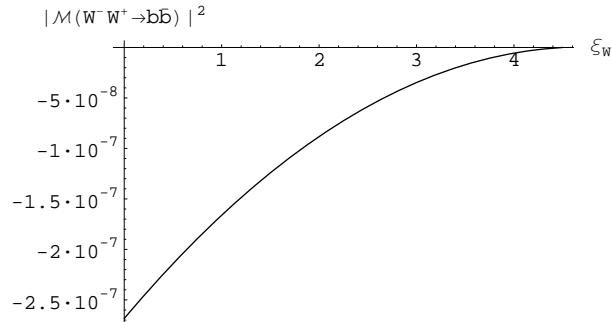


FIG. 7: Gauge dependence of two-loop $|\mathcal{M}(W^-W^+ \rightarrow b\bar{b})|^2$ in on-shell mass renormalization scheme with Higgs mass 120Gev.

the data: $x_p = 1$, $x_E = 4$, $e = 0.3028$, $s_w^2 = 0.2312$, $m_W = 80.42\text{Gev}$, $m_u = 3\text{Mev}$, $m_c = 1.25\text{Gev}$, $m_t = 174.3\text{Gev}$, $m_d = 6\text{Mev}$, $m_s = 120\text{Mev}$, $m_b = 4.2\text{Gev}$, $|V_{ub}| = 0.004$, $|V_{cb}| = 0.040$, $|V_{td}| = 0.009$, $|V_{ts}| = 0.039$ and $|V_{tb}| = 0.999$ [15]. Contrarily, from Eq.(16) one readily find that the branch cut containing the function $\theta[m_t - m_{down-quark} - \sqrt{\xi_W}m_W]$ of the two-loop cross section of the physical process $W^-W^+ \rightarrow b\bar{b}$ is gauge independent under the pole mass renormalization scheme.

IV. CONCLUSION

We have discussed the gauge dependence of fermion mass definition under the on-shell and pole mass renormalization schemes. Through the calculation of top quark's two-loop mass counterterm we strictly prove that the fermion mass definition is gauge dependent under the on-shell mass renormalization scheme at the first time. This leads to the physical result obtained by the on-shell mass renormalization scheme also gauge dependent. On the contrary, we don't find such gauge dependence in the pole mass renormalization scheme. Besides, the gauge-dependent difference of the physical result between the two mass renormalization schemes cannot be neglected at two-loop level. Therefore we should use the pole mass renormalization scheme rather than the on-shell mass renormalization scheme to calculate physical results beyond one-loop level.

Acknowledgments

The author thanks Prof. Xiao-Yuan Li and Prof. Cai-dian Lu for the useful guidance.

Appendix

In this appendix we list the ξ_W -dependent contributions of the possible cuts of Fig.3 to Eq.(5). We firstly calculate the ξ_W -dependent contribution of the possible cut of the first topology of Fig.3 to Eq.(5). Using the cutting rules of

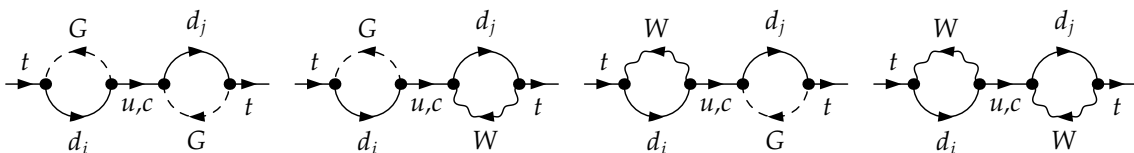


FIG. 8: Diagrams of top quark's self energy of the first topology of Fig.3.

Ref.[12] we obtain the ξ_W -dependent contribution of the cuts of Fig.8 to Eq.(5):

$$\begin{aligned}
& \frac{m_t}{2} \text{Re}[\Sigma^L(m_t^2) + \Sigma^R(m_t^2) + \Sigma^{S,L}(m_t^2) + \Sigma^{S,R}(m_t^2)]_{\xi_W\text{-cut}} \\
&= \frac{e^4 m_W}{8192 \pi^2 s_w^4 x_t^{5/2}} \sum_{i=d,s,b} |V_{3i}|^2 B_i(x_t - \xi_W - x_i) (B_i x_t (x_t - \xi_W - x_i) - 2A_i C_i + 2 \sum_{j=d,s,b} |V_{3j}|^2 A_j C_j) \\
&\times \theta[m_t - m_i - \sqrt{\xi_W m_W}] - \frac{e^4 m_W}{8192 \pi^2 s_w^4 x_t^{3/2}} \sum_{i,j=d,s,b} |V_{3i}|^2 |V_{3j}|^2 B_i B_j (x_t - \xi_W - x_i) (x_t - \xi_W - x_j) \\
&\times \theta[m_t - m_i - \sqrt{\xi_W m_W}] \theta[m_t - m_j - \sqrt{\xi_W m_W}]. \tag{19}
\end{aligned}$$

Since there isn't four-particle-interaction vertex including fermion in standard model, the second, 3th and 4th topologies of Fig.3 cannot contribute to Eq.(5). So we don't need to consider their contributions.

The top quark's self-energy diagrams of the 5th topology of Fig.3 which satisfy the cutting conditions of Fig.4 are shown in Fig.9. Using the cutting rules we obtain the ξ_W -dependent contribution of the cuts of Fig.9 to Eq.(5):

$$\begin{aligned}
& \frac{m_t}{2} \text{Re}[\Sigma^L(m_t^2) + \Sigma^R(m_t^2) + \Sigma^{S,L}(m_t^2) + \Sigma^{S,R}(m_t^2)]_{\xi_W} \\
&= -\frac{e^4 m_W}{8192 \pi^2 s_w^2 x_t^{3/2}} (\xi_W^3 - 3\xi_W^2 - 9\xi_W + 11) \theta[1 - \xi_W] \sum_{i=d,s,b} |V_{3i}|^2 A_i C_i \\
&+ \frac{3e^4 m_W}{8192 \pi^2 s_w^2 x_t^{3/2} \xi_W^2} (\xi_W - 1)^3 \theta[\xi_W - 1] \sum_{i=d,s,b} |V_{3i}|^2 B_i \\
&\times (x_i^2 - (2x_t + \xi_W)x_i + x_t(x_t - \xi_W)) \theta[m_t - m_i - \sqrt{\xi_W m_W}] \\
&+ \frac{3e^4 m_W}{8192 \pi^2 c_w^4 s_w^4 x_t^{3/2} \xi_W^2} D^3 \theta[\sqrt{\xi_W} - 1/c_w - 1] \sum_{i=d,s,b} |V_{3i}|^2 B_i \\
&\times (x_i^2 - (2x_t + \xi_W)x_i + x_t(x_t - \xi_W)) \theta[m_t - m_i - \sqrt{\xi_W m_W}], \tag{20}
\end{aligned}$$

where

$$D = ((\xi_W - 1)^2 c_w^4 - 2(\xi_W + 1)c_w^2 + 1)^{1/2}. \tag{21}$$

Here we have restricted ourselves to $\xi_W > 0$ [4] and used the present experiment result $m_t < m_H + m_W$ [16].

Lastly we calculate the ξ_W -dependent contribution of the possible cut of the 6th topology of Fig.3 to Eq.(5). We will calculate the contributions of the five cuts of Fig.5 one by one. Firstly we calculate the ξ_W -dependent contribution of the first cut of Fig.5 to Eq.(5). The result is

$$\begin{aligned}
& \frac{m_t}{2} \text{Re}[\Sigma^L(m_t^2) + \Sigma^R(m_t^2) + \Sigma^{S,L}(m_t^2) + \Sigma^{S,R}(m_t^2)]_{\xi_W\text{-cut}} \\
&= \frac{e^4 m_W}{8192 \pi^2 s_w^4 x_t^{5/2}} \sum_{i=d,s,b} |V_{3i}|^2 (x_t - \xi_W - x_i) (2A_i B_i C_i - x_t(x_t - \xi_W - x_i) B_i^2) \theta[m_t - m_i - \sqrt{\xi_W m_W}]. \tag{22}
\end{aligned}$$

We note that in the calculation of Eq.(22) we have given the photon an infinitesimal mass λ in order to regularize the result of the diagrams the 5th propagator of which is photon (see Fig.3). The result of each such diagram contains the term $\ln \lambda$, but the total contribution of them to Eq.(5) is zero as shown in Eq.(22). Because we find that none of the diagram in Fig.10 satisfies the cutting condition of the second cut of Fig.5, the contribution of the second cut of Fig.5 to Eq.(5) is zero. Similarly, the contribution of the 4th cut of Fig.5 to Eq.(5) is also zero due to the same reason. For the contribution of the third cut of Fig.5 to Eq.(5) we have

$$\begin{aligned}
& \frac{m_t}{2} \text{Re}[\Sigma^L(m_t^2) + \Sigma^R(m_t^2) + \Sigma^{S,L}(m_t^2) + \Sigma^{S,R}(m_t^2)]_{\xi_W\text{-cut}} \\
&= \frac{e^4 m_W}{16384 \pi^2 s_w^2 x_t^{3/2}} \sum_{i=d,s,b} |V_{3i}|^2 A_i C_i (\xi_W^3 - 3\xi_W^2 - 9\xi_W + 11) \theta[1 - \xi_W] \\
&- \frac{3e^4 m_W}{16384 \pi^2 s_w^2 x_t^{3/2} \xi_W^2} (\xi_W - 1)^3 \theta[\xi_W - 1] \sum_{i=d,s,b} \frac{|V_{3i}|^2}{B_i} (x_t^4 - (3\xi_W + 4x_i)x_t^3)
\end{aligned}$$

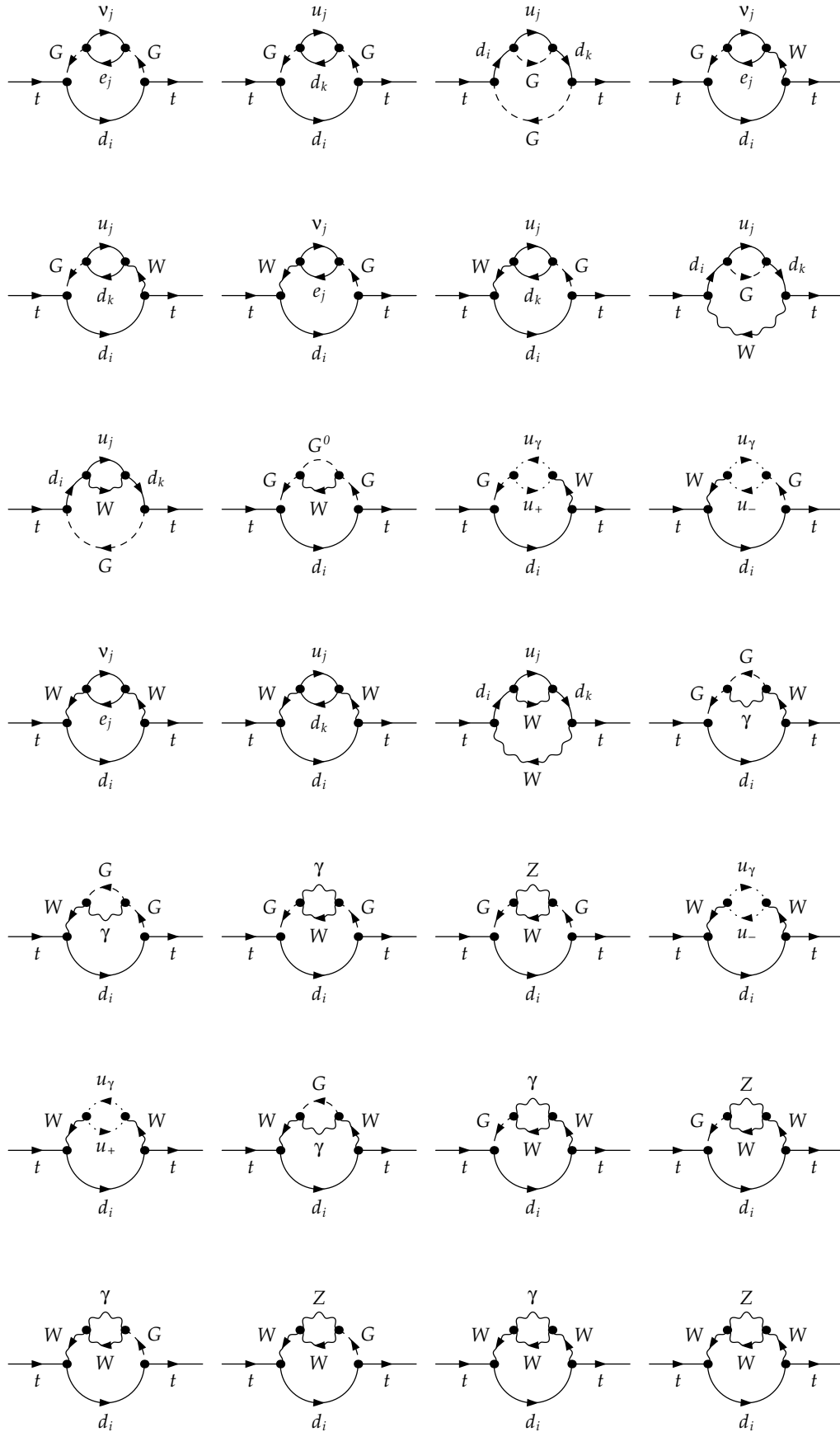


FIG. 9: Diagrams of top quark's self energy of the 5th topology of Fig.3 which satisfy the cutting conditions of Fig.4.

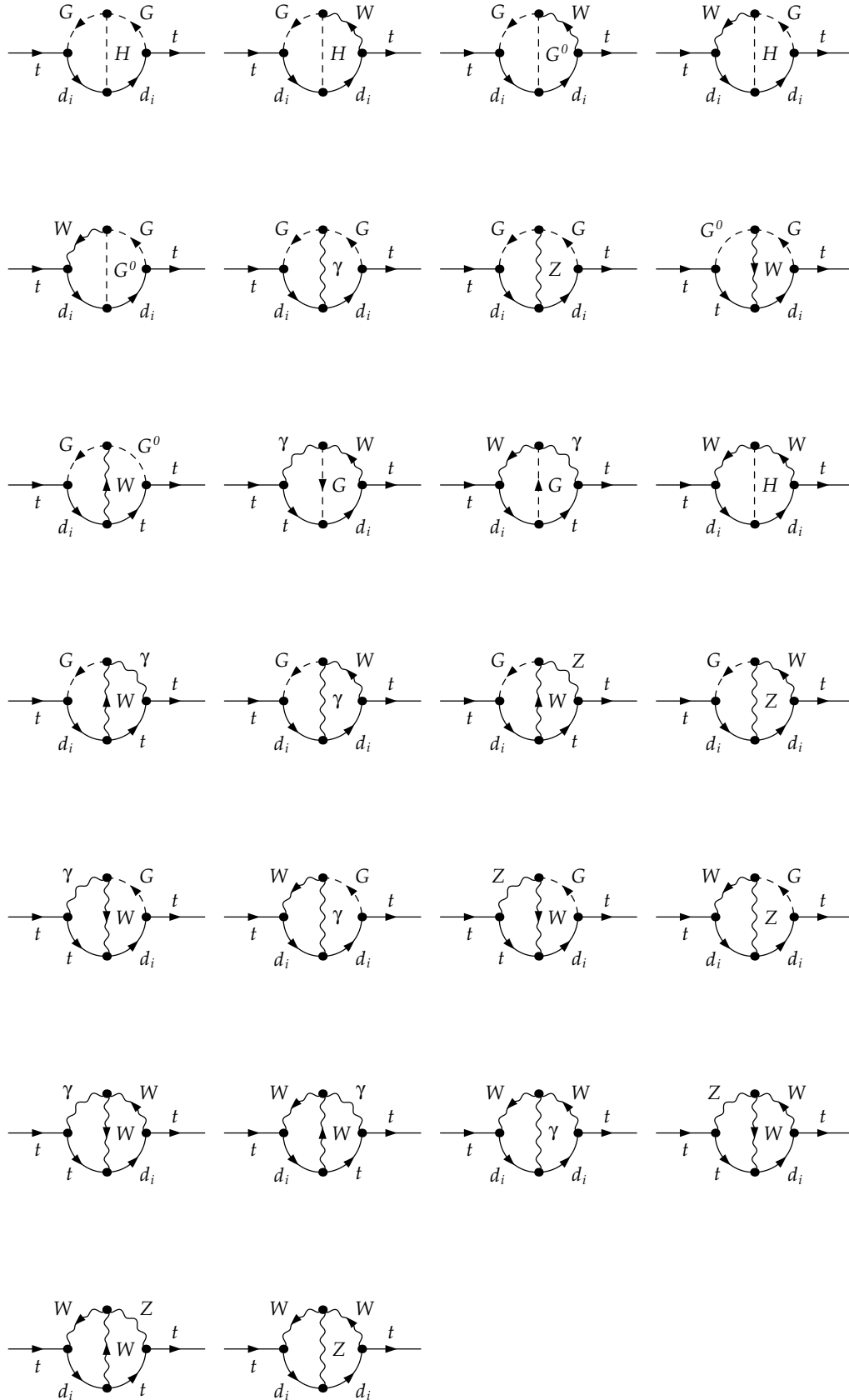


FIG. 10: Diagrams of top quark's self energy of the 6th topology of Fig.3 which satisfy the cutting conditions of Fig.5.

$$\begin{aligned}
& + 3(\xi_W^2 + x_i \xi_W + 2x_i^2)x_t^2 - (\xi_W^3 - 2x_i \xi_W^2 - 3x_i^2 \xi_W + 4x_i^3)x_t - (\xi_W - x_i)^3 x_i \theta[m_t - m_i - \sqrt{\xi_W} m_W] \\
& - \frac{3e^4 m_W}{16384 \pi^2 c_w^4 s_w^4 x_t^{3/2} \xi_W^2} D^3 \theta[\sqrt{\xi_W} - 1/c_w - 1] \sum_{i=d,s,b} \frac{|V_{3i}|^2}{B_i} (x_t^4 - (3\xi_W + 4x_i)x_t^3 \\
& + 3(\xi_W^2 + x_i \xi_W + 2x_i^2)x_t^2 - (\xi_W^3 - 2x_i \xi_W^2 - 3x_i^2 \xi_W + 4x_i^3)x_t - (\xi_W - x_i)^3 x_i) \theta[m_t - m_i - \sqrt{\xi_W} m_W]. \quad (23)
\end{aligned}$$

For the contribution of the 5th cut of Fig.5 to Eq.(5) we obtain the same result as Eq.(23). One can also see this point from the left-and-right symmetry of the 3th and 5th cuts of Fig.5.

Summing up all of the above results we obtain the ξ_W -dependent contribution of the cuts of Fig.3 to Eq.(5). The result has been shown in Eq.(13). From Eqs.(19-23) one also readily see that the total contribution of CKM matrix elements of each topology of Fig.3 to Eq.(5) is real number.

-
- [1] M. Veltman, *Physica* **29** (1963) 186;
D. Bardin and G. Passarino, *The Standard Model in the Making Precision Study of the Electroweak Interactions*, Oxford Science Pub., Clarendon Press, Oxford, 1999;
D. Espriu, J. Manzano and P. Talavera, *Phys. Rev. D* **66** (2002) 076002.
 - [2] A. Denner, *Fortschr. Phys.* **41** (1993) 307.
 - [3] A. Sirlin, *Phys. Rev. Lett.* **67** (1991) 2127; *Phys. Lett. B* **267** (1991) 240;
R.G. Stuart, *Phys. Lett. B* **272** (1991) 353.
 - [4] M. Passera, A. Sirlin, *Phys. Rev. Lett.* **77** (1996) 4146;
B.A. Kniehl, A. Sirlin, *Phys. Rev. Lett.* **81** (1998) 1373;
P.A. Grassi, B.A. Kniehl and A. Sirlin, *Phys. Rev. Lett.* **86** (2001) 389;
M.L. Nekrasov, *Phys. Lett. B* **531** (2002) 225;
B.A. Kniehl, A. Sirlin, *Phys. Lett. B* **530** (2002) 129.
 - [5] P. Gambino, P.A. Grassi, *Phys. Rev. D* **62** (2000) 076002.
 - [6] D. Espriu, J. Manzano and P. Talavera, *Phys. Rev. D* **66** (2002) 076002;
Y. Zhou, *J. Phys. G* **29** (2003) 1031.
 - [7] A. Bednyakov, A. Sheplyakov, *Phys. Lett. B* **604** (2004) 91.
 - [8] N.K. Nielsen, *Nucl. Phys. B* **101** (1975) 173;
R. Tarrach, *Nucl. Phys. B* **183** (1981) 384;
O. Piguet and K. Sibold, *Nucl. Phys. B* **253** (1985) 517.
 - [9] J. Kublbeck, M. Bohm, A. Denner, *Comput. Phys. Commun.* **60** (1990) 165;
G.J. van Oldenborgh, J.A.M. Vermaseren, *Z. Phys. C* **46** (1990) 425;
T. Hahn, M. Perez-Victoria, *Comput. Phys. Commun.* **118** (1999) 153.
 - [10] G. Passarino, M. Veltman, *Nucl. Phys. B* **160** (1979) 151;
G. 't Hooft, M. Veltman, *Nucl. Phys. B* **135** (1979) 365.
 - [11] R.E. Cutkosky, *J. Math. Phys.* **1**, 429 (1960).
 - [12] Y. Zhou, hep-ph/0508225.
 - [13] N. Cabibbo, *Phys. Rev. Lett.* **10**, 531 (1963);
M. Kobayashi and K. Maskawa, *Prog. Theor. Phys.* **49** (1973) 652.
 - [14] Yong Zhou, hep-ph/0508227.
 - [15] *The European Physical Journal C*, **15** (2000) 1-878.
 - [16] PDG 2004, S. Eidelman et al., *Phys. Lett. B* **592** (2004) 1.